Localization of a Gene for Nonsyndromic Renal Hypodysplasia to Chromosome 1p32-33

Simone Sanna-Cherchi, Gianluca Caridi, Patricia L. Weng, Monica Dagnino, Marco Seri, Anita Konka, Danio Somenzi, Alba Carrea, Claudia Izzi, Domenica Casu, Landino Allegri, Kai M. Schmidt-Ott, Jonathan Barasch, Francesco Scolari, Roberto Ravazzolo, Gian Marco Ghiggeri, and Ali G. Gharavi

Nonsyndromic defects in the urinary tract are the most common cause of end-stage renal failure in children and account for a significant proportion of adult nephropathy. The genetic basis of these disorders is not fully understood. We studied seven multiplex kindreds ascertained via an index case with a nonsyndromic solitary kidney or renal hypodysplasia. Systematic ultrasonographic screening revealed that many family members harbor malformations, such as solitary kidneys, hypodysplasia, or ureteric abnormalities (in a total of 29 affected individuals). A genomewide scan identified significant linkage to a 6.9-Mb segment on chromosome 1p32-33 under an autosomal dominant model with reduced penetrance (peak LOD score 3.5 at *D1S2652* in the largest kindred). Altogether, three of the seven families showed positive LOD scores at this interval, demonstrating heterogeneity of the trait (peak HLOD 3.9, with 45% of families linked). The chromosome 1p32-33 interval contains 52 transcription units, and at least 23 of these are expressed at stage E12.5 in the murine ureteric bud and/or metanephric mesenchyme. These data show that autosomal dominant nonsyndromic renal hypodysplasia and associated urinary tract malformations are genetically heterogeneous and identify a locus for this common cause of human kidney failure.

The human kidney is composed of 500,000 to 1.8 million independent functional units, called "nephrons."[1,2] Kidney failure occurs when acquired or hereditary disorders cause progressive nephron loss and reduce their numbers to below the threshold required for maintenance of fluid-electrolyte homeostasis and elimination of nitrogenous wastes. Congenital abnormalities that impair nephron development comprise 30%–50% of congenital anomalies detected on prenatal screening.[3,4] There is wide interindividual variability in the anatomy and clinical course of these malformations, but, altogether, they account for up to 50% of pediatric and 10% of adult end-stage renal disease worldwide.[5,6] Renal agenesis/adysplasia (MIM %191830) is one of the most severe forms of malformations; bilateral renal agenesis occurs in ∼1 in 2,000 births and is nearly always fatal because of oligohydramnios and consequent pulmonary hypoplasia.[3,4,7,8] Other related phenotypic variants, such as unilateral agenesis and unilateral or bilateral renal hypodysplasia, occur more frequently (1 in 1,000 births).[3,4] Affected kidneys frequently exhibit dysplastic parenchyma, reduced nephron mass, and impaired function, predisposing the individual to renal failure.[8] Kidney malformations are also commonly accompanied by anatomic abnormalities in the lower urinary tract, such as ureteropelvic junction obstruction (UPJO) or vesicoureteral reflux (VUR).[8–12] Impairment of urinary drainage due to these lower-tract defects further contributes to nephron injury and augments the risk of chronic renal failure.

The etiology of the majority of nonsyndromic forms of urinary tract malformations remains unknown. The overlap in phenotypic expression, together with the limitations of morphological classification, has complicated efforts to understand the primary pathogenesis of these disorders and to formulate clear diagnostic categories. For example, it is not known whether the observation of a congenital solitary kidney in an adult represents a primary failure of kidney development (agenesis) or the end-result of a dysplastic kidney that underwent involution.[3,8] Several risk factors for human urinary tract malformations are recognized, including maternal diabetes[13] or intrauterine exposure to drugs such as ACE inhibitors.[14] In addition, the genetic bases for several rare, syndromic disorders featuring renal developmental defects have been elucidated (e.g., renal-coloboma syndrome [MIM #120330], Fraser syndrome [MIM #219000], and branchiootorenal syndrome [MIM #113650]). Gene-targeting studies have shown that alteration in gene dosage or disruption in the temporospatial sequence of gene expression in intermediate mesodermal tissues (the metanephric

mesenchyme [MM] or the ureteric bud [UB]) can result in developmental defects that affect both the upper and lower urinary system.[8,12,15–22] Moreover, because of interdependence of developmental pathways, similar renal and urologic phenotypes arise by inactivation of different genes.[8,12,15–22] These findings are consistent with the "bud theory" of Mackie and Stephens, which proposes that abnormalities in the kidney and ureter stem from the same common mechanism—namely, abnormal ureteral budding from the Wolffian duct into the bladder results in malposition of the ureteral orifice.[12] These data together with the phenotypic overlap observed in human renal and urologic disorders emphasize the potential for genetic heterogeneity of disease. Candidate-gene screening has confirmed heterogeneity, revealing mutations in the *Uroplakin 3A* gene in a subset of patients with renal dysplasia.[23,24] Other recent surveys of patients with renal hypodysplasia, many of whom had extra-renal defects suggestive of syndromic disease, identified mutations in *PAX2, TCF2, EYA1, SIX1,* or *SALL1* in up to 17%–25% of patients.[25,26] Thus, mutations identified to date account for a fraction of nonsyndromic renal developmental defects, leaving the majority of cases unexplained.

Several studies have reported familial aggregation of nonsyndromic renal malformations. For example, ultrasonographic screening of first-degree relatives of 41 index patients with bilateral renal agenesis/dysgenesis identified asymptomatic renal malformations (mostly unilateral renal agenesis) in 9% of relatives.[9] Additional malformations were also documented, including UPJO and VUR. This increased recurrence risk among relatives has been confirmed in several other studies and is estimated at 4%–20%.[9–11,27] Multigenerational occurrence of disease has suggested multifactorial or dominant inheritance in most kindreds,[9–11] but families with probable recessive inheritance have also been reported.[27] Altogether, these data strongly argue in favor of genetic causation and suggest that familial aggregation is under-recognized because anatomical defects in many family members are often silent. No linkage studies in such families have been reported to date.

We set out to investigate the genetic basis of nonsyndromic urinary tract malformations. Our previous studies of primary VUR had suggested that gene mapping for such heterogeneous disorders would necessitate large numbers of medium-sized pedigrees or uniquely large kindreds.[28] In the situation of uncertainty about clinical classification and the potential for genetic heterogeneity, we strived to assemble a cohort with a strong genetic contribution by concentrating on patients with the most severe clinical phenotype—namely, solitary kidneys and/or renal hypodysplasia. We identified seven Italian pedigrees ascertained through an index patient with solitary kidney/hypodysplasia documented by a renal sonogram and/or isotopic scintigraphy (fig. 1). Solitary kidney was diagnosed when one kidney only was seen in the imaging study. Hypodysplasia was defined as kidney length below the 95% tolerance limit based on height- and weight-adjusted sonographic nomograms.[29,30] A pediatric nephrologist and clinical geneticist with expertise in diagnosis of developmental disorders of the urinary tract evaluated all the patients. Histories and physical examinations were conducted to search for evidence of multiorgan malformations, which would suggest syndromic forms of renal hypodysplasia. In particular, we focused on the possibility of disease associated with *PAX2* or *TCF2* mutations, which may masquerade as nonsyndromic malformations.[25,26] We performed ophthalmologic exams to search for retinal colobomas and investigated the presence of deafness or genital malformations, which would be indicative of renal-coloboma syndrome. In addition, we searched for abnormalities suggestive of *TCF2* mutations, such as presence of renal cysts, diabetes, and elevated liver enzymes or uric acid levels. The exclusion of *PAX2* and *TCF2* by clinical criteria was further confirmed by linkage analysis in all pedigrees and by direct sequencing of *TCF2* exons in one kindred (K101) that had a minimally positive LOD score at the *TCF2* locus. There was also no history of intrauterine exposure to teratogenic agents, such as ACE inhibitors and angiotensin receptor antagonists, and no history of maternal diabetes.

To detect additional affected relatives, we performed ultrasonographic screening and chart review of family members. We identified 22 family members with anatomic abnormalities (table 1). Most family members had congenital solitary kidneys/hypodysplasia, but other abnormalities were also identified, such as UPJO (11 individuals), VUR (6 individuals), infundibulopelvic stenosis (1 individual), and multicystic dysplastic kidney (1 individual). These additional defects mostly presented in association with the hypodysplasia phenotype but also occurred in isolation in a few family members (table 1). One individual (31 in K100, age 10 years) had asymmetric kidney sizes that fell within the normal range, but she was classified as affected because she had an MZ twin with unilateral renal hypodysplasia (this individual and her twin were considered a single affected individual in the genome scan).

Altogether, 29 individuals were classified as affected on the basis of abnormal urinary anatomy seen on imaging studies (12 males and 17 females, listed in table 1). Of these affected individuals, 10 were asymptomatic and received a diagnosis at the time of screening, and 5 had renal dysfunction (as defined by serum creatinine >1.5 mg/dl) or had developed end-stage renal failure requiring dialysis or transplantation. Twenty-nine family members had normal imaging studies and normal renal function and were classified as unaffected (fig. 1). In addition, chart review revealed that five other family members had died in childhood from end-stage renal failure, but renal imaging studies for these individuals were not available to make a definitive diagnosis (fig. 1). These individuals and all other family members who did not undergo imaging studies were considered to have an unknown phenotype. All phenotypes were assigned prospectively. In these ped-
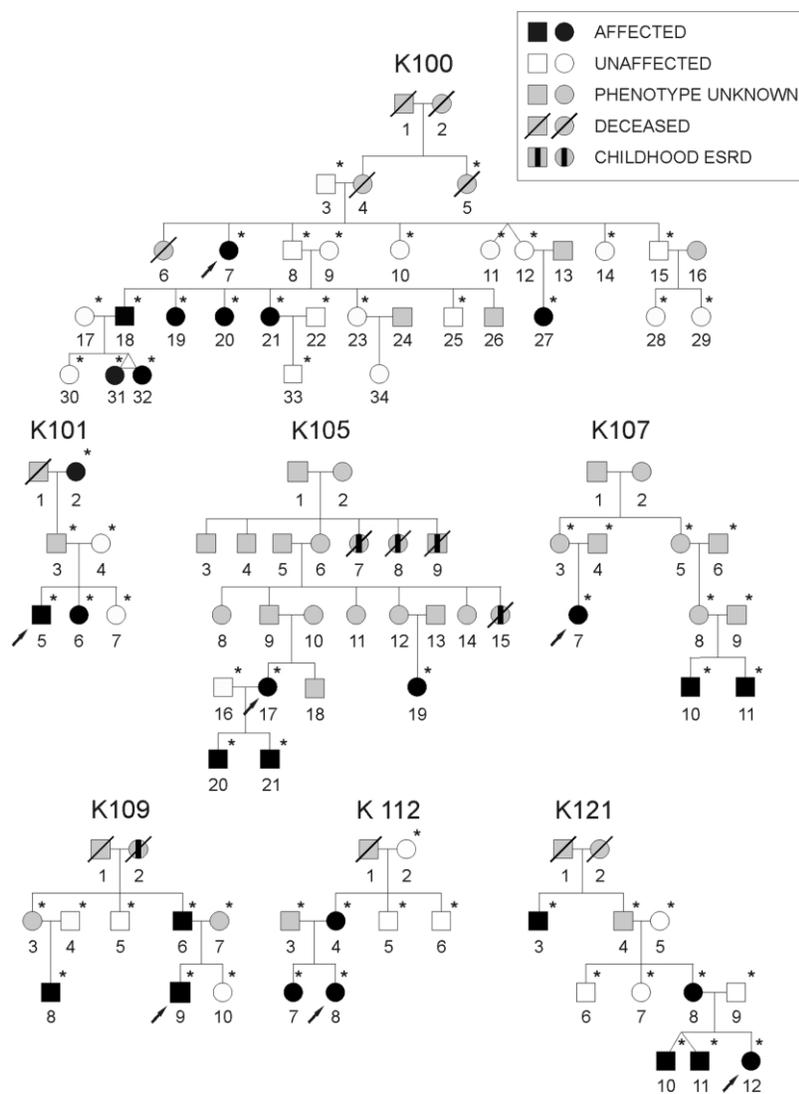
Figure 1. Pedigree structure of the seven families studied. Patients with childhood end-stage renal disease (ESRD) but no sonographic data available are indicated by a blackened rectangle inside the symbol. Arrows identify the index cases. Asterisks (*) mark the individuals from whom DNA was available for the study. Individual identification numbers correspond to table 1.

igrees, the mode of inheritance was most consistent with multifactorial inheritance or autosomal dominant transmission with incomplete penetrance.

All individuals gave informed consent, and the study protocol was approved by the Western Institutional Review Board for Columbia University and the ethics committee at the Gaslini Institute. Total genomic DNA was isolated from peripheral white blood cells by use of standard procedures. Genomewide screens were performed with two independent methodologies. In the largest kindred (K100), we performed an ~10-cM microsatellite screen of autosomes (382 markers from Linkage Mapping Set v2.5 MD10 [Applied Biosystems]), using seven affected and seven unaffected individuals. The seven unaffected individuals (8, 10, 11, 12, 14, 15, and 23) were included, to increase inheritance information. During that time, ge-

nomewide SNP genotyping technology became readily available. We therefore genotyped all affected individuals from our seven kindreds for 10,204 SNPs, using the GeneChips Mapping 10K 2.0 Arrays (Affymetrix). DNA processing and gene-chip hybridization were performed as suggested by Affymetrix. This provided a uniform data set across all pedigrees.

We performed pairwise analysis of linkage, using FAST-LINK 4.1,[31] and multipoint analysis, using ALLEGRO 1.2c[32] and Simwalk 2.89.[33] Parametric analysis was performed under a model of autosomal dominant transmission with reduced penetrance (85%, estimated from the pedigrees), disease-gene frequency of 0.001, and phenocopy rate of 0.001. We computed parametric LOD scores under genetic homogeneity and heterogeneity (calculation of HLODs). Nonparametric statistics were concurrently computed

Table 1. Clinical Data of the Affected Individuals from the Seven Pedigrees

| Pedigree and Individual	Sex	Age (years)	Kidney Phenotype	Kidney Length[a] R/L (cm)	Associated Defect	Chronic Renal Failure	Dialysis
K100:							
7	F	55	Solitary kidney	-/12	None	No	No
18	M	36	Hypodysplasia (R)	6/12.3	None	No	No
19	F	38	Hypodysplasia (R+L)	7/5.5	None	Yes	Yes
20	F	32	Hypodysplasia (R+L)	6/5.8	UPJO (L)	Yes	Yes
21	F	28	Hypodysplasia (R+L)	5/5.5	UPJO (L)	Yes	Yes
27	F	12	Infundibulopelvic stenosis (R)	10.5/10.8	Hydro-calix (R)	No	No
31	F	10	Asymmetric sizes	11/8.5	None	No	No
32	F	10	Hypodysplasia (R)	6/10.5	None	No	No
K101:							
2	F	82	Hypodysplasia (R+L)	5/6	ND	Yes	Yes
5	M	15	Hypodysplasia (R)	7/10.9	UPJO (R) and VUR (R+L)	No	No
6	F	23	Normal kidney size	11/10.5	UPJO (L)	No	No
K105:							
17	F	37	Solitary kidney	12/-	None	No	No
19	F	35	Hypodysplasia (R)	6/11	None	No	No
20	M	16	Normal kidney size	10/10.8	VUR (R+L)	No	No
21	M	14	Normal kidney size	9.8/10	MCDK (L) and VUR (L)	No	No
K107:							
7	F	40	Hypodysplasia (R)	6/10.8	VUR (R)	No	No
10	M	10	Hypodysplasia (R+L)	7/5.3	VUR (L)	No	No
11	M	13	Hypodysplasia (R+L)	8.8/6.4	VUR (L)	No	No
K109:							
6	M	48	Normal kidney size	12/12.2	UPJO (L)	No	No
8	M	18	Normal kidney size	11.5/12	UPJO (R)	No	No
9	M	19	Hypodysplasia (R)	6/12	UPJO (R)	No	No
K112:							
4	F	60	Normal kidney size	12.5/12.3	UPJO (L)	No	No
7	F	28	Normal kidney size	11.5/12	UPJO (R)	No	No
8	F	30	Hypodysplasia (R+L)	8/7	UPJO (R)	Yes	No
K121:							
3	M	80	Solitary kidney	12/-	None	No	No
8	F	28	Normal kidney size	12/12.5	UPJO (L)	No	No
10	M	6	Hypodysplasia (L)	10/5	None	No	No
11	M	6	Solitary kidney	11/-	None	No	No
12	F	.3	Solitary kidney	-/9	None	No	No

NOTE.—R = right; L = left; MCDK = multicystic dysplastic kidney; ND = not determined.

[a] A hyphen (-) indicates that the kidney was not visualized. For reference, the normal range for kidney size in an adult is 10–15 cm; the 95th percentile interval for a 10-year-old is 7–11 cm.

with Allegro (the NPL score and associated exact *P* value). Allele frequencies were calculated on the basis of the frequencies observed in the data set for the microsatellites; for the SNP data, frequencies were based on public, ethnically matched, frequencies provided by Affymetrix. Published thresholds for suggestive and significant linkage were used.[34,35] To detect our study power, 200 simulations under the assumption of linkage with 85% penetrance were performed using the SLINK program.[36] The simulated pedigrees were next tested for linkage by use of the autosomal dominant model delineated above. This analysis demonstrated a maximal expected LOD score of 4.1 (average 3.1 ± 1.3) in K100.

We therefore initially focused on K100, because this pedigree was sufficiently large to localize a trait locus independently. With analysis of affected individuals only (hereafter, "affected-only analysis"), several loci showed LOD scores >1 in K100 for both microsatellite and SNP analyses: 1p32-33 (LOD = 1.4), 1q31-33 (LOD = 1.5), and 6p24-25 (LOD = 1.5) (fig. 2). When the phenotype of unaffected individuals was introduced into the analysis (with the microsatellite scan), the LOD increased to 2.7 at the chromosome 1p32-33 interval (*D1S2770*) but decreased at the other two intervals. Together, these data suggested that the linkage peak on chromosome 1p32-33 was unlikely to be an artifactual finding produced by linkage disequilibrium between SNP markers. We genotyped 42 additional microsatellite markers across these three promising intervals and genotyped all 16 available family members to extract full inheritance information. After the incorporation of microsatellite markers, we achieved inheritance information >0.9 at these loci. Evidence of linkage to chromosomes 1q31-33 and 6p24-25 became less significant (LOD ≤ 1.2). However, the LOD score on chromosome 1p32-33 improved significantly, resulting in a peak parametric LOD score of 3.5 between *D1S2652* and
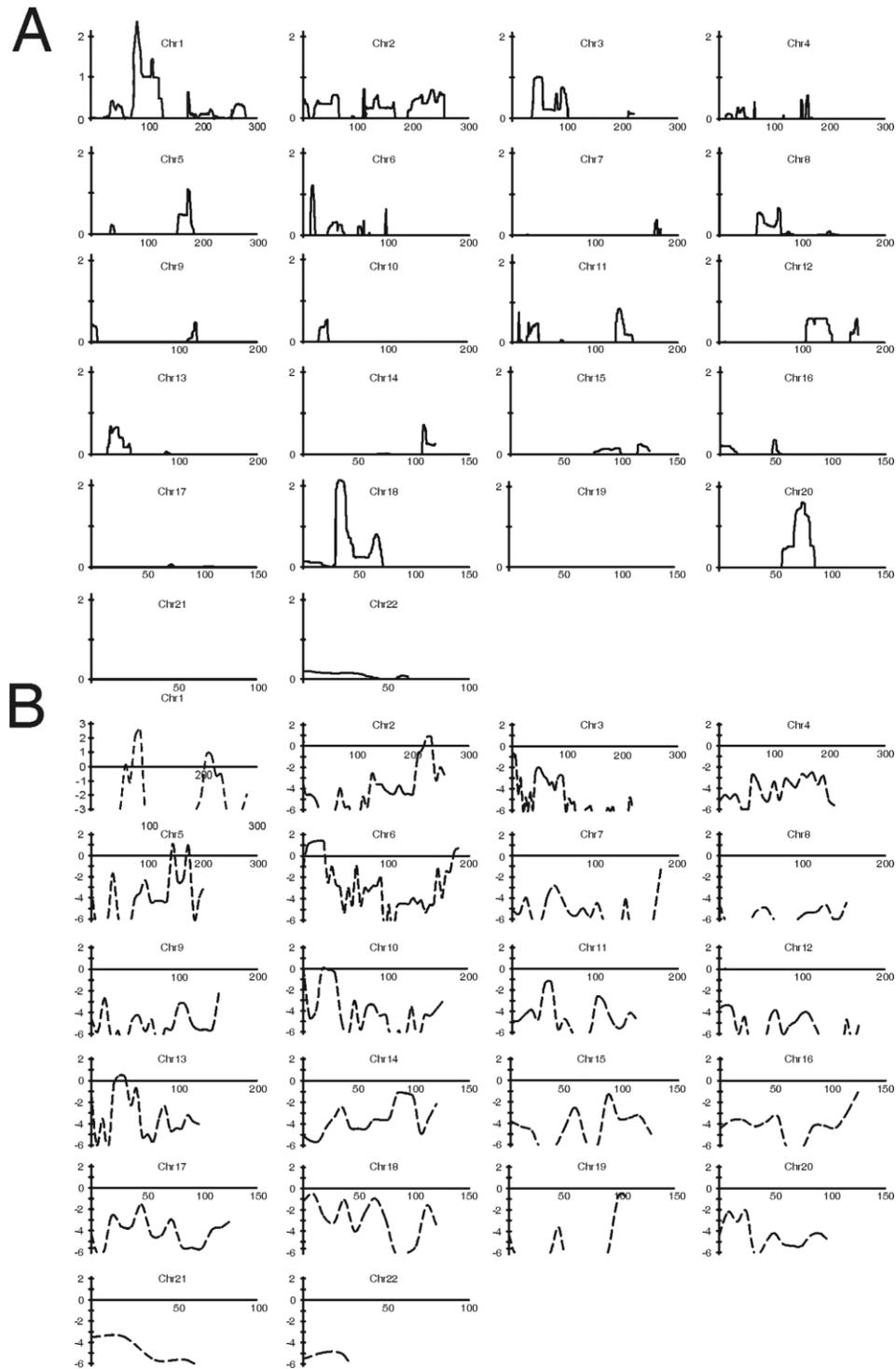
Figure 2. LOD score distribution across the genome. The continuous lines (*A*) represent the HLOD scores obtained from the SNP scan with affected-only analysis of all seven pedigrees (minimum HLOD = 0). The dashed lines (*B*) represent the parametric LOD scores obtained from microsatellite scan in pedigree K100 alone. Values <−6 are not shown. Chr = chromosome.

rs1341347 (fig. 3). The likelihood of linkage to 1p32-33 was 200-fold greater than the next most likely interval at 1q31-33 (LOD = 1.2). As shown in table 2, these results were robust to changes in estimates of disease-allele frequencies (0.001–0.01), penetrances (65%–95%), and phenocopy rates (0.001–0.01). This analysis therefore achieved genomewide significance on the basis of published criteria[34,35] and established localization of a gene for nonsyndromic renal hypodysplasia on chromosome 1p32-33 (fig. 3).

We next determined whether our six other pedigrees with renal hypodysplasia demonstrate linkage to this interval. After genotyping 24 microsatellites across 1p32-33 in these remaining pedigrees, affected-only analysis provided an HLOD of 1.1 (with 45% of families linked) and an NPL of 2.2 (*P* = .02) at 1p32-33, demonstrating that some but not all families linked to this interval. Two kindreds (K105 and K109) showed near-maximal expected LOD scores between *D1S200* and *D1S220,* encompassing the same linkage interval as K100. In these two kindreds, the conditional probability of linkage to 1p32-33 was >0.95 (table 3). In K112, a LOD score of 0.3 was achieved by affected-only analysis, but it decreased to −0.6 when the phenotype of unaffected individuals was introduced in the calculations. Results for the other three kindreds (K101, K107, and K121) were negative in the affected-only analysis and after incorporation of unaffected phenotypes. To further verify that the data for the kindreds with positive LOD scores point to the same interval as K100, we combined all seven families and analyzed linkage to 1p32-33 under a model of locus heterogeneity. This analysis resulted in a peak HLOD of 3.9 with 45% of families linked; this HLOD peak coincides perfectly with the LOD curve obtained with K100 alone (fig. 3). As before, varying linkage parameters had little effect on the HLOD results (table 2), exceeding the threshold for genomewide significance in all cases.[34,35] Finally, evidence of linkage to 1p32-33 was also supported by nonparametric analysis (NPL = 5.3; *P* = 1.5 × 10⁻⁴). Altogether, these data provide genomewide evidence for localization of a gene for renal hypodysplasia on 1p32-33 and confirm that this trait is genetically heterogeneous.

We next analyzed the 1p32-33 haplotypes, which are defined by 51 SNP and microsatellite markers across our linked interval. This demonstrated that all affected members and obligate carriers of K100, K105, and K109 inherited the linked haplotypes at 1p32-33 (fig. 4). Consistent with incomplete penetrance of the trait, one unaffected member in pedigree K100 (individual 15) had inherited the linked haplotype, and his unaffected daughter (individual 28) had inherited the distal portion of the haplotype. The recombination interval, inferred from affected-only analysis, localizes the disease gene within the 6.9-Mb region between *D1S2661* and *D1S203,* corresponding to the region with the maximal LOD scores from SNP and microsatellite analysis. Comparison of haplotypes showed no evidence of shared segments between the three families
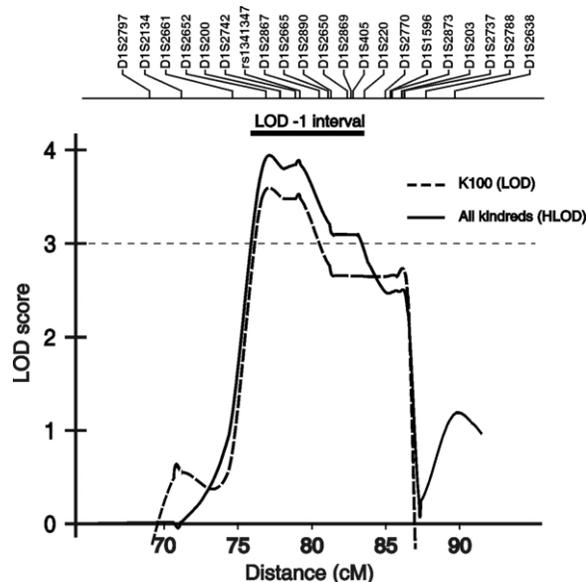
Figure 3. LOD plot of chromosome 1p32-33 locus. The multipoint LOD score in K100 and the HLOD in all seven pedigrees combined are shown. The X-axis shows genetic distance based on the deCODE map. The location of microsatellite markers genotyped is shown above the graph. The LOD-1 support interval is indicated by the thick horizontal bar above the LOD curve.

with positive LOD scores on 1p32-33, suggesting independent mutations. This is not surprising, because K100 originates from Sardinia, whereas the other two kindreds belong to other regions of Italy.

Examination of genes located within the LOD-1 interval on 1p32-33 (by use of the NCBI Map Viewer, build 36.1; Ensembl, v39; and University of California–Santa Cruz [UCSC] Genome Browser, March 2006 assembly) reveals 52 transcription units, of which 23 encode hypothetical or predicted proteins. None of the positional candidates have been previously implicated in structural abnormalities of the kidney or urologic tract. Consultation of Online Mendelian Inheritance of Man (OMIM) revealed that mutations in six positional candidates have been implicated in human traits (*PCSK9, BSDN, C8A, C8B, TACSTD2,* and *DHCR24*). Mice carrying null alleles for seven other genes (*HOOK1, DAB1, JUN, PRKAA2, PPAP2B, DHCR24,* and *SSBP3*) have also been reported, but none feature urogenital defects. Two other genes on 1p32-33 had been associated with kidney developmental defects (*FOXD2* and *CPT2*) but were located outside our recombinant interval.[37,38]

A powerful method to annotate positional candidates is to determine their expression pattern within relevant tissues and developmental time points. Nephron development is a recursive process that starts in the 2nd month of gestation, when the UB invades the MM, initiating branching morphogenesis.[21,22] Genetic manipulations in mice have shown that inactivation of genes expressed in

Table 2. Multipoint LOD Scores on Chromosome 1p32-33 with Varying Linkage Parameters

Penetrances (%)	LOD for K100 at			HLOD at		
	Disease-Allele Frequency .001		Disease-Allele Frequency .01 and Phenocopy Rate .001	Disease-Allele Frequency .001		Disease-Allele Frequency .01 and Phenocopy Rate .001
	Phenocopy Rate .001	Phenocopy Rate .01		Phenocopy Rate .001	Phenocopy Rate .01	
65	3.2	3.2	3.2	3.6	3.5	3.3
75	3.4	3.4	3.4	3.7	3.7	3.5
85	3.5	3.5	3.5	3.9	3.8	3.6
95	3.3	3.3	3.3	3.7	3.7	3.4

NOTE.—Peak parametric HLODs are shown for all seven pedigrees combined (with 45% of families linked).

either compartment can produce the renal hypodysplasia phenotype.[12–20] Hence, one can predict that the phenotype observed in our families originates from dysregulation of a gene that is normally expressed early in nephrogenesis but could be localized to the MM, the UB, or both. Accordingly, we performed annotation of positional candidates with the results of a recently published study that characterized gene expression in the murine MM, UB tips, and UB stalk.[39] This expression profiling was performed at the E12.5 time point, corresponding to the 2nd and 3rd round of cleavage in branching morphogenesis, among the earliest time points at which the MM can be anatomically differentiated from the UB in the mouse. We particularly focused on genes that show differential expression in UB tips, which coordinate UB branching and secrete factors necessary for nephron induction in the MM. Examination of the data revealed that 30 positional candidates had murine homologs and corresponding probe sets on the arrays; of these, 23 had detectable expression in the developing MM, UB tip, or UB stalk (table 3). Among positional candidates, three genes initially stood out because they had high expression levels across metanephric compartments (*JUN* and *HOOK1*) or displayed UB-specific expression in mouse (*TACSTD2*). *JUN*, a component of the AP-1 transcription factor complex, is essential for cell proliferation and organogenesis after midgestation.[40] It acts downstream of RET signaling and may modify UB branching and nephrogenesis.[41] *HOOK1* is a microtubule-binding protein involved in endocytosis in *Drosophila* and is responsible for the abnormal spermatozoon head shape phenotype in mice.[42] *TACSTD2* encodes a cell-surface receptor recognized as a carcinoma-associated antigen, with mutations associated with gelatinous drop-like corneal dystrophy.[43] *TACSTD2* and *TACSTD1* were identified as UB-specific secreted proteins in multiple studies; alteration in *TACSTD2* may therefore modify UB branching and nephrogenesis.[39,44] We performed direct sequencing of the coding exons of the *JUN, HOOK1, TACSTD2, FOXD2,* and *CPT2* genes, using the index patients from our linked families, but found no evidence of pathogenic mutations.

We also tested whether the 1p32-33 interval may be relevant to inherited disorders that affect the ureters but not the kidneys. This search was motivated by the possibility that primary ureteric defects can produce chronic renal parenchymal injury and subsequent involution of the kidneys, resulting in the finding of small kidney size on sonogram. We tested linkage to 1p32-33 in 10 families segregating isolated ureteric abnormalities (7 kindreds with primary VUR,[28] 2 multiplex kindreds with isolated UPJO, and 1 family with duplicated collecting system). All individuals in this second cohort had normal kidney size. Parametric linkage analysis was performed with 20 microsatellite loci spanning to 1p32-33, under the same model used to map the hypodysplasia pedigrees (affected-only analysis). We found no evidence for linkage to 1p32-33 in these kindreds. Moreover, our 1p32-33 interval is > 90 Mb proximal to, and therefore distinct from, the 1p13 locus reported elsewhere for linkage to primary VUR and reflux nephropathy.[45] These data suggest the 1p32-33 interval harbors a gene that may be specific to familial disorders that feature the renal hypodysplasia phenotype.

Because several families displayed negative LOD scores on 1p32-33, we searched for additional loci across the genome that account for disease. As K100 clearly linked to 1p32-33, we performed genomewide analysis of linkage after removing this kindred from our cohort (affected-only analysis with SNPs). There was no evidence of linkage across the genome under a model of genetic homogeneity. Under a model of locus heterogeneity, we identified several linkage peaks with HLOD >1 on chromosomes 18p11-q11, 20q11-13, 1p32-33, and 3p21-22. We next added 40 additional markers at these four loci and typed all available family members, to yield inheritance information >0.9. After this analysis, only the HLOD signal on chromosome 3p21-22 improved (HLOD 1.5; $\alpha = 0.35$; NPL = 2.3; $P = .02$; maximum between *D3S1768* and *D3S2409*). These data indicate that, other than 1p32-33, there are no significant intervals across the genome that account for the trait in remaining families (table 4).

In this study, we performed detailed phenotypic characterization of families with nonsyndromic renal hypodysplasia, identified a locus for this trait, and completed the initial steps for functional annotation and prioritization of positional candidates. Because of the complex signaling network involved in urogenital development, renal

Table 3. List of Positional Candidates with Detectable Expression in the Developing Murine Urinary Tract

| Human Gene Symbol	Human Gene Description	Mus Gene Symbol	Affymetrix ProbeSet	MM[a]	UB Tip[a]	UB Stalk[a]
YIPF1	Yip1 domain family, member 1	Yipf1	1424196_at	270	288	284
C1ORF41	Chromosome 1 ORF 41	2900042B11Rik	1453016_at	390	248	398
LRRC42	Leucine-rich repeat containing 42	Lrrc42	1424049_at	394	442	419
TMEM59	Transmembrane protein 59	Tmem59	1450046_at	13	17	13
C1orf83	Chromosome 1 ORF 83	2210012G02Rik	1418662_at	141	148	143
MRPL37	Mitochondrial ribosomal protein L37	Mrpl37	1423764_s_at	385	494	400
SSBP3	Single-stranded DNA binding protein 3	Ssbp3	1425940_a_at	217	148	225
			1427917_s_at	985	805	954
ACOT11	Acyl-CoA thioesterase 11	Acot11	1429267_at	95	76	104
C1orf179	Chromosome 1 ORF 179	BC026682	1417443_at	55	52	52
TTC4	Tetratricopeptide repeat domain 4	Ttc4	1451193_x_at	528	523	518
			1451192_a_at	549	497	539
PARS2	Prolyl-tRNA synthetase (mitochondrial) (putative)	Pars2	1427309_at	203	203	208
			1418130_at	132	153	112
PCSK9	Proprotein convertase subtilisin/kexin type 9 AD hypercholesterolemia	Pcsk9	1437453_s_at	18	48	27
USP24	Ubiquitin-specific protease 24	Usp24	1452868_at	209	287	263
			1448013_at	178	259	244
			1448014_s_at	124	171	138
			1441018_at	40	35	35
PPAP2B	Phosphatidic acid phosphatase type 2B	Ppap2b	1429514_at	673	488	738
			1448908_at	545	390	623
PRKAA2	Protein kinase, AMP-activated, alpha	Prkaa2	1429463_at	28	52	45
DAB1	Disabled homolog 1 (*Drosophila*)	Dab1	1427308_at	31	47	37
			1427307_a_at	66	90	71
			1421100_a_at	11	16	12
			1435578_s_at	25	40	38
			1435577_at	15	18	18
OMA1	OMA1 homolog, zinc metallopeptidase (*S. cerevisiae*)	Oma1	1424299_at	199	246	214
TACSTD2	Tumor-associated calcium signal transducer 2	Tacstd2	1423323_at	11	535	523
MYSM1	Myb-like, SWIRM and MPN domains 1	Mysm1	1437202_at	118	110	142
JUN	V-jun sarcoma virus 17 oncogene homolog (avian)	Jun	1417409_at	2,347	2,774	3,758
			1448694_at	1,137	1,119	1,866
FLJ10986	Hypothetical protein FLJ10986	2310009E04Rik	1452799_at	102	114	108
HOOK1	Hook homolog 1 (*Drosophila*)	Hook1	1438018_at	252	881	446
			1439173_at	18	56	27
CYP2J2	Cytochrome P450, family 2, subfamily J, polypeptide 2	Cyp2j6	1417952_at	51	121	117

NOTE.—Genes reported to be present in at least one compartment are shown.

[a] The last three columns show raw expression levels across metanephric compartments (from Schmidt-Ott et al.[39]).

developmental phenotypes are likely to display a high degree of genetic heterogeneity, necessitating large numbers of pedigrees or uniquely large kindreds for gene mapping.[28] We therefore performed systematic sonographic screening of families with renal hypodysplasia, to extend kindreds and maximize study power. We confirmed that this phenotype segregates as an autosomal dominant trait with reduced penetrance. Next, genomewide analysis of linkage demonstrated that this trait is genetically heterogeneous, with about half of families showing linkage to a 6.9-Mb interval on 1p32-33. This linkage assignment is firmly established by a large family (K100), which provided evidence for genomewide significance on its own.

Our present findings can be pursued by several approaches. We can perform systematic sequencing of all positional candidates to identify the pathogenic mutations. However, further prioritization of candidates may help accelerate gene identification. This can be achieved by determining renal gene expression at multiple developmental time points and by examining tissue and cell-specific expression through in situ hybridization. In addition, our largest kindred (K100) is of Sardinian origin, providing the opportunity to refine the interval by disequilibrium mapping. Sardinia is composed of subpopulations that descend from limited sets of ancestors and exhibit strong linkage disequilibrium.[46] This characteristic has facilitated gene identification for several traits, such as uric acid nephrolithiasis.[47] Hence, comparison of the haplotypes between K100 and Sardinian patients from the same locality may identify chromosomal segments inher-
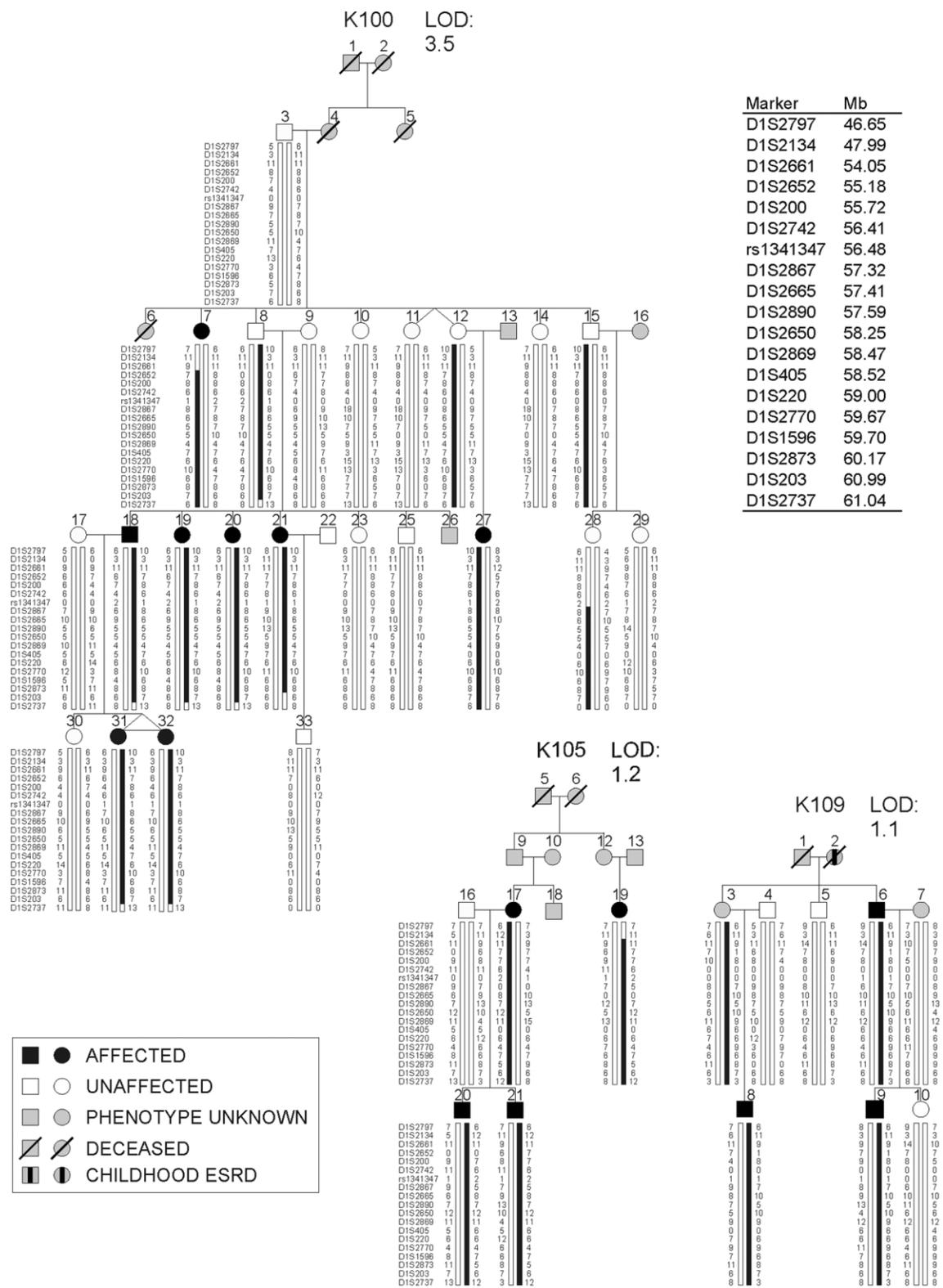
Figure 4. Haplotype structure of the three pedigrees that show linkage to the 1p32-33 locus. Genotypes for the most informative markers spanning the linkage interval are shown (19 of 51 SNPs and microsatellite loci genotyped are shown). The vertical bars highlight the linked (*black*) and the wild-type (*white*) haplotypes. The physical locations of the markers are indicated in a list at the top right. Patients with childhood end-stage renal disease (ESRD) but no sonographic data available are indicated by a blackened rectangle inside the symbol.

Table 4. Multipoint Parametric LOD Scores at the Most Significant Intervals in the Seven Pedigrees

Kindred	LOD			
	1p32-33[a]	3p21-22[b,e]	18p11-q11[c,e]	20q11-13[d,e]
100	3.5	−4	−2.6	−5
101	−2.5	−1.3	−2.8	.8
105	1.2	−1.3	1	−2
107	−1.4	1.2	1.2	1.2
109	1.1	−2.4	−.5	−1.9
112	−.6	−.4	.4	.6
121	−2.3	1.8	−.5	−3

[a] HLOD = 3.9 (45% of families linked).
[b] HLOD = 1.5 (35% of families linked).
[c] HLOD = 1.2 (50% of families linked).
[d] HLOD = 1 (35% of families linked).
[e] HLOD was calculated without K100 because this kindred shows significant linkage to chromosome 1p32-33.

ited by descent and help refine the interval to a limited set of candidates.

Identification of the gene underlying the 1p32-33 linkage will provide insight into the molecular basis of renal developmental disorders and will help improve diagnostic schemes. Low nephron number at birth and consequent low renal reserve have been proposed as a major susceptibility factor for the development of nephropathy or hypertension.[48,49] Some genes regulating kidney development may also participate in tissue repair after renal injury.[50] This suggests that identification of the 1p32-33 hypodysplasia gene may also inform us about interindividual variability in nephron number and have additional diagnostic or therapeutic implications.

Web Resources

The URLs for data presented herein are as follows:

Ensembl, http://www.ensembl.org/Homo_sapiens/index.html (for v39)
NCBI Map Viewer, http://www.ncbi.nlm.nih.gov/mapview/ (for build 36.1)
Online Mendelian Inheritance in Man (OMIM), http://www.ncbi.nlm.nih.gov/Omim/ (for renal agenesis/adysplasia, renal-coloboma syndrome, Fraser syndrome, and branchiootorenal syndrome)
UCSC Genome Browser, http://genome.ucsc.edu/cgi-bin/hgGateway (for March 2006 assembly)

References

1. Hughson M, Farris AB 3rd, Douglas-Denton R, Hoy WE, Bertram JF (2003) Glomerular number and size in autopsy kidneys: the relationship to birth weight. Kidney Int 63:2113–2122
2. Hughson MD, Douglas-Denton R, Bertram JF, Hoy WE (2006) Hypertension, glomerular number, and birth weight in African Americans and white subjects in the southeastern United States. Kidney Int 69:671–678
3. Hiraoka M, Tsukahara H, Ohshima Y, Kasuga K, Ishihara Y, Mayumi M (2002) Renal aplasia is the predominant cause of congenital solitary kidneys. Kidney Int 61:1840–1844
4. Helin I, Persson PH (1986) Prenatal diagnosis of urinary tract abnormalities by ultrasound. Pediatrics 78:879–883
5. US Renal Data System (2005) USRDS 2005 annual data report: atlas of end-stage renal disease in the United States. National Institutes of Health, National Institute of Diabetes and Digestive and Kidney Diseases, Bethesda, MD
6. Ardissino G, Dacco V, Testa S, Bonaudo R, Claris-Appiani A, Taioli E, Marra G, Edefonti A, Sereni F (2003) Epidemiology of chronic renal failure in children: data from the ItalKid project. Pediatrics 111:e382–e387
7. Stroup NE, Edmonds L, O'Brien TR (1990) Renal agenesis and dysgenesis: are they increasing? Teratology 42:383–395
8. Woolf AS, Price KL, Scambler PJ, Winyard PJ (2004) Evolving concepts in human renal dysplasia. J Am Soc Nephrol 15:998–1007
9. Roodhooft AM, Birnholz JC, Holmes LB (1984) Familial nature of congenital absence and severe dysgenesis of both kidneys. N Engl J Med 310:1341–1345
10. McPherson E, Carey J, Kramer A, Hall JG, Pauli RM, Schimke RN, Tasin MH (1987) Dominantly inherited renal adysplasia. Am J Med Genet 26:863–872
11. Carter CO, Evans K, Pescia G (1979) A family study of renal agenesis. J Med Genet 16:176–188
12. Mackie GG, Stephens FD (1975) Duplex kidneys: a correlation of renal dysplasia with position of the ureteral orifice. J Urol 114:274–280
13. Parikh CR, McCall D, Engelman C, Schrier RW (2002) Congenital renal agenesis: case-control analysis of birth characteristics. Am J Kidney Dis 39:689–694
14. Cooper WO, Hernandez-Diaz S, Arbogast PG, Dudley JA, Dyer S, Gideon PS, Hall K, Ray WA (2006) Major congenital malformations after first-trimester exposure to ACE inhibitors. N Engl J Med 354:2443–2451
15. Vize PD, Woolf AS, Bard JBL (2003) The kidney: from normal development to congenital disease. Elsevier Science, San Diego, CA
16. Grieshammer U, Le M, Plump AS, Wang F, Tessier-Lavigne M, Martin GR (2004) SLIT2-mediated ROBO2 signaling restricts kidney induction to a single site. Dev Cell 6:709–717
17. Yu J, McMahon AP, Valerius MT (2004) Recent genetic studies of mouse kidney development. Curr Opin Genet Dev 14:550–557
18. Miyazaki Y, Oshima K, Fogo A, Ichikawa I (2003) Evidence that bone morphogenetic protein 4 has multiple biological functions during kidney and urinary tract development. Kidney Int 63:835–844
19. Durbec P, Marcos-Gutierrez CV, Kilkenny C, Grigoriou M, Wartiowaara K, Suvanto P, Smith D, Ponder B, Costantini F,

Saarma M, et al (1996) GDNF signalling through the Ret receptor tyrosine kinase. Nature 381:789–793

20. Torres M, Gomez-Pardo E, Dressler GR, Gruss P (1995) Pax-2 controls multiple steps of urogenital development. Development 121:4057–4065

21. Schmidt-Ott KM, Lan D, Hirsh BJ, Barasch J (2006) Dissecting stages of mesenchymal-to-epithelial conversion during kidney development. Nephron Physiol 104:p56–p60

22. Vainio S, Lin Y (2002) Coordinating early kidney development: lessons from gene targeting. Nat Rev Genet 3:533–543

23. Jenkins D, Bitner-Glindzicz M, Malcolm S, Hu CC, Allison J, Winyard PJ, Gullett AM, Thomas DF, Belk RA, Feather SA, et al (2005) De novo Uroplakin IIIa heterozygous mutations cause human renal adysplasia leading to severe kidney failure. J Am Soc Nephrol 16:2141–2149

24. Schonfelder EM, Knuppel T, Tasic V, Miljkovic P, Konrad M, Wuhl E, Antignac C, Bakkaloglu A, Schaefer F, Weber S (2006) Mutations in Uroplakin IIIA are a rare cause of renal hypodysplasia in humans. Am J Kidney Dis 47:1004–1012

25. Weber S, Moriniere V, Knuppel T, Charbit M, Dusek J, Ghiggeri GM, Jankauskiene A, Mir S, Montini G, Peco-Antic A, et al (2006) Prevalence of mutations in renal developmental genes in children with renal hypodysplasia: results of the ESCAPE study. J Am Soc Nephrol 17:2864–2870

26. Ulinski T, Lescure S, Beaufils S, Guigonis V, Decramer S, Morin D, Clauin S, Deschenes G, Bouissou F, Bensman A, et al (2006) Renal phenotypes related to hepatocyte nuclear factor-1beta (TCF2) mutations in a pediatric cohort. J Am Soc Nephrol 17:497–503

27. Pasch A, Hoefele J, Grimminger H, Hacker HW, Hildebrandt F (2004) Multiple urinary tract malformations with likely recessive inheritance in a large Somalian kindred. Nephrol Dial Transplant 19:3172–3175

28. Sanna-Cherchi S, Reese A, Hensle T, Caridi G, Izzi C, Kim YY, Murer L, Scolari F, Ravazzolo R, Ghiggeri GM, Gharavi AG (2005) Familial vesicoureteral reflux: testing replication of linkage in seven new multigenerational kindreds. J Am Soc Nephrol 16:1781–1787

29. Dinkel E, Ertel M, Dittrich M, Peters H, Berres M, Schulte-Wissermann H (1985) Kidney size in childhood: sonographical growth charts for kidney length and volume. Pediatr Radiol 15:38–43

30. Han BK, Babcock DS (1985) Sonographic measurements and appearance of normal kidneys in children. AJR Am J Roentgenol 145:611–616

31. Cottingham RW Jr, Idury RM, Schaffer AA (1993) Faster sequential genetic linkage computations. Am J Hum Genet 53:252–263

32. Gudbjartsson DF, Jonasson K, Frigge ML, Kong A (2000) Allegro, a new computer program for multipoint linkage analysis. Nat Genet 25:12–13

33. Sobel E, Lange K (1996) Descent graphs in pedigree analysis: applications to haplotyping, location scores, and marker-sharing statistics. Am J Hum Genet 58:1323–1337

34. Faraway JJ (1993) Distribution of the admixture test for the detection of linkage under heterogeneity. Genet Epidemiol 10:75–83

35. Lander E, Kruglyak L (1995) Genetic dissection of complex traits: guidelines for interpreting and reporting linkage results. Nat Genet 11:241–247

36. Ott J (1989) Computer-simulation methods in human linkage analysis. Proc Natl Acad Sci USA 86:4175–4178

37. Bonnefont JP, Djouadi F, Prip-Buus C, Gobin S, Munnich A, Bastin J (2004) Carnitine palmitoyltransferases 1 and 2: biochemical, molecular and medical aspects. Mol Aspects Med 25:495–520

38. Kume T, Deng K, Hogan BL (2000) Minimal phenotype of mice homozygous for a null mutation in the forkhead/winged helix gene, Mf2. Mol Cell Biol 20:1419–1425

39. Schmidt-Ott KM, Yang J, Chen X, Wang H, Paragas N, Mori K, Li JY, Lu B, Costantini F, Schiffer M, et al (2005) Novel regulators of kidney development from the tips of the ureteric bud. J Am Soc Nephrol 16:1993–2002

40. Johnson RS, van Lingen B, Papaioannou VE, Spiegelman BM (1993) A null mutation at the c-jun locus causes embryonic lethality and retarded cell growth in culture. Genes Dev 7:1309–1317

41. Jijiwa M, Fukuda T, Kawai K, Nakamura A, Kurokawa K, Murakumo Y, Ichihara M, Takahashi M (2004) A targeting mutation of tyrosine 1062 in Ret causes a marked decrease of enteric neurons and renal hypoplasia. Mol Cell Biol 24:8026–8036

42. Mendoza-Lujambio I, Burfeind P, Dixkens C, Meinhardt A, Hoyer-Fender S, Engel W, Neesen J (2002) The Hook1 gene is non-functional in the abnormal spermatozoon head shape (azh) mutant mouse. Hum Mol Genet 11:1647–1658

43. Tsujikawa M, Kurahashi H, Tanaka T, Nishida K, Shimomura Y, Tano Y, Nakamura Y (1999) Identification of the gene responsible for gelatinous drop-like corneal dystrophy. Nat Genet 21:420–423

44. Caruana G, Cullen-McEwen L, Nelson AL, Kostoulias X, Woods K, Gardiner B, Davis MJ, Taylor DF, Teasdale RD, Grimmond SM, et al (2006) Spatial gene expression in the T-stage mouse metanephros. Gene Expr Patterns 6:807–825

45. Feather SA, Malcolm S, Woolf AS, Wright V, Blaydon D, Reid CJ, Flinter FA, Proesmans W, Devriendt K, Carter J, et al (2000) Primary, nonsyndromic vesicoureteric reflux and its nephropathy is genetically heterogeneous, with a locus on chromosome 1. Am J Hum Genet 66:1420–1425

46. Angius A, Bebbere D, Petretto E, Falchi M, Forabosco P, Maestrale B, Casu G, Persico I, Melis PM, Pirastu M (2002) Not all isolates are equal: linkage disequilibrium analysis on Xq13.3 reveals different patterns in Sardinian sub-populations. Hum Genet 111:9–15

47. Gianfrancesco F, Esposito T, Ombra MN, Forabosco P, Maninchedda G, Fattorini M, Casula S, Vaccargiu S, Casu G, Cardia F, et al (2003) Identification of a novel gene and a common variant associated with uric acid nephrolithiasis in a Sardinian genetic isolate. Am J Hum Genet 72:1479–1491

48. Brenner BM, Chertow GM (1994) Congenital oligonephropathy and the etiology of adult hypertension and progressive renal injury. Am J Kidney Dis 23:171–175

49. Keller G, Zimmer G, Mall G, Ritz E, Amann K (2003) Nephron number in patients with primary hypertension. N Engl J Med 348:101–108

50. Mori K, Lee HT, Rapoport D, Drexler IR, Foster K, Yang J, Schmidt-Ott KM, Chen X, Li JY, Weiss S, et al (2005) Endocytic delivery of lipocalin-siderophore-iron complex rescues the kidney from ischemia-reperfusion injury. J Clin Invest 115:610–621